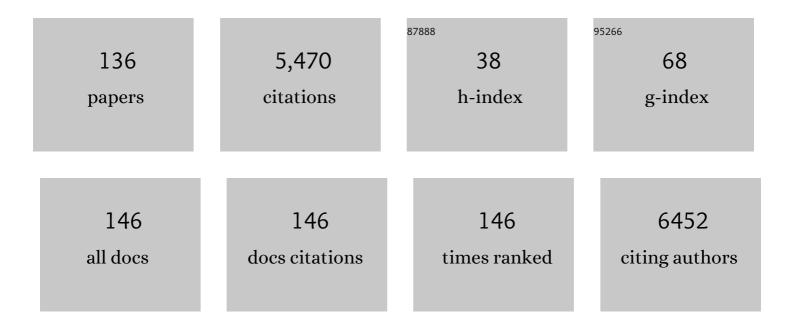
## Takashi Toyao

List of Publications by Year in descending order

Source: https://exaly.com/author-pdf/5297262/publications.pdf Version: 2024-02-01



TAKASHI TOVAO

#	Article	IF	CITATIONS
1	Ga speciation and ethane dehydrogenation catalysis of Ga-CHA and MOR: Comparative investigation with Ga-MFI. Catalysis Today, 2023, 411-412, 113824.	4.4	5
2	Propane Dehydrogenation Catalysis of Titanium Hydrides: Positive Effect of Hydrogen Co-feeding. Chemistry Letters, 2022, 51, 88-90.	1.3	2
3	High-loading Ga-exchanged MFI zeolites as selective and coke-resistant catalysts for nonoxidative ethane dehydrogenation. Catalysis Science and Technology, 2022, 12, 986-995.	4.1	9
4	Machine Learning Analysis of Literature Data on the Water Gas Shift Reaction toward Extrapolative Prediction of Novel Catalysts. Chemistry Letters, 2022, 51, 269-273.	1.3	7
5	Role of Ba in an Al <sub>2</sub> O <sub>3</sub> â€Supported Pdâ€based Catalyst under Practical Threeâ€Way Catalysis Conditions. ChemCatChem, 2022, 14, .	3.7	4
6	Catalytic Methylation of Benzene over Pt/MoOx/TiO2 and Zeolite Catalyst Using CO2 and H2. Chemistry Letters, 2022, 51, 149-152.	1.3	1
7	Continuous CO <sub>2</sub> Capture and Selective Hydrogenation to CO over Na-Promoted Pt Nanoparticles on Al <sub>2</sub> O <sub>3</sub> . ACS Catalysis, 2022, 12, 2639-2650.	11.2	22
8	Understanding and controlling the formation of surface anion vacancies for catalytic applications. Catalysis Science and Technology, 2022, 12, 2398-2410.	4.1	2
9	Experimental and Theoretical Investigation of Metal–Support Interactions in Metal-Oxide-Supported Rhenium Materials. Journal of Physical Chemistry C, 2022, 126, 4472-4482.	3.1	5
10	Mechanistic study on three-way catalysis over Pd/La/Al2O3 with high La loading. Catalysis Today, 2022, , .	4.4	1
11	Enhancement of the hydrodesulfurization and Câ~'S bond cleavage activities of rhodium phosphide catalysts by platinum addition. Journal of Catalysis, 2022, 408, 294-302.	6.2	8
12	Redox-Driven Reversible Structural Evolution of Isolated Silver Atoms Anchored to Specific Sites on γ-Al <sub>2</sub> O <sub>3</sub> . ACS Catalysis, 2022, 12, 544-559.	11.2	16
13	Effect of oxygen storage materials on the performance of Pt-based three-way catalysts. Catalysis Science and Technology, 2022, 12, 3534-3548.	4.1	6
14	Oxidation Catalysis over Solid-State Keggin-Type Phosphomolybdic Acid with Oxygen Defects. Journal of the American Chemical Society, 2022, 144, 7693-7708.	13.7	30
15	Super Mg <sup>2+</sup> Conductivity around 10 <sup>–3</sup> S cm <sup>–1</sup> Observed in a Porous Metal–Organic Framework. Journal of the American Chemical Society, 2022, 144, 8669-8675.	13.7	17
16	Catalytic Decomposition of N <sub>2</sub> 0 in the Presence of O <sub>2</sub> through Redox of Rh Oxide in a RhO <sub><i>x</i></sub> /ZrO <sub>2</sub> Catalyst. ACS Catalysis, 2022, 12, 6325-6333.	11.2	14
17	Trends in Surface Oxygen Formation Energy in Perovskite Oxides. ACS Omega, 2022, 7, 18427-18433.	3.5	2
18	Layered silicate stabilises diiron to mimic UV-shielding TiO2 nanoparticle. Materials Today Nano, 2022, 19, 100227.	4.6	5

Τακάσηι Τογάο

#	Article	IF	CITATIONS
19	Application to Electroluminescence Devices with Dimethylformamide-Stabilized Niobium Oxide Nanoparticles. ACS Applied Nano Materials, 2022, 5, 7658-7663.	5.0	2
20	<i>N</i> , <i>N</i> -Dimethylformamide-stabilized ruthenium nanoparticle catalyst for β-alkylated dimer alcohol formation <i>via</i> Guerbet reaction of primary alcohols. RSC Advances, 2022, 12, 16599-16603.	3.6	2
21	<i>In Situ</i> Spectroscopic Studies of the Redox Catalytic Cycle in NH <sub>3</sub> –SCR over Chromium-Exchanged Zeolites. Journal of Physical Chemistry C, 2022, 126, 11082-11090.	3.1	7
22	Mechanism of Standard NH <sub>3</sub> –SCR over Cu-CHA via NO <sup>+</sup> and HONO Intermediates. Journal of Physical Chemistry C, 2022, 126, 11594-11601.	3.1	10
23	In situ/operando spectroscopic studies on NH3–SCR reactions catalyzed by a phosphorus-modified Cu-CHA zeolite. Catalysis Today, 2021, 376, 73-80.	4.4	12
24	Kinetic and spectroscopic insights into the behaviour of Cu active site for NH3-SCR over zeolites with several topologies. Catalysis Science and Technology, 2021, 11, 2718-2733.	4.1	10
25	High dimensionally structured W-V oxides as highly effective catalysts for selective oxidation of toluene. Catalysis Today, 2021, 363, 60-66.	4.4	6
26	Greener and facile synthesis of Cu/ZnO catalysts for CO2 hydrogenation to methanol by urea hydrolysis of acetates. RSC Advances, 2021, 11, 14323-14333.	3.6	6
27	Hydrolysis of amides to carboxylic acids catalyzed by Nb <sub>2</sub> O <sub>5</sub> . Catalysis Science and Technology, 2021, 11, 1949-1960.	4.1	18
28	Reverse Water-Gas Shift Reaction via Redox of Re Nanoclusters Supported on TiO2. Chemistry Letters, 2021, 50, 158-161.	1.3	11
29	Surface activation by electron scavenger metal nanorod adsorption on TiH <sub>2</sub> , TiC, TiN, and Ti <sub>2</sub> O <sub>3</sub> . Physical Chemistry Chemical Physics, 2021, 23, 16577-16593.	2.8	9
30	Bulk tungsten-substituted vanadium oxide for low-temperature NOx removal in the presence of water. Nature Communications, 2021, 12, 557.	12.8	92
31	Reverse water-gas shift reaction over Pt/MoO <sub>x</sub> /TiO <sub>2</sub> : reverse Mars–van Krevelen mechanism <i>via</i> redox of supported MoO <sub>x</sub> . Catalysis Science and Technology, 2021, 11, 4172-4180.	4.1	20
32	Local structure and NO adsorption/desorption property of Pd <sup>2+</sup> cations at different paired Al sites in CHA zeolite. Physical Chemistry Chemical Physics, 2021, 23, 22273-22282.	2.8	15
33	Factors determining surface oxygen vacancy formation energy in ternary spinel structure oxides with zinc. Physical Chemistry Chemical Physics, 2021, 23, 23768-23777.	2.8	12
34	Alkyl decorated metal–organic frameworks for selective trapping of ethane from ethylene above ambient pressures. Dalton Transactions, 2021, 50, 10423-10435.	3.3	15
35	Transformation of Bulk Pd to Pd Cations in Small-Pore CHA Zeolites Facilitated by NO. Jacs Au, 2021, 1, 201-211.	7.9	34
36	Effect of Oxygen Vacancies on Adsorption of Small Molecules on Anatase and Rutile TiO <sub>2</sub> Surfaces: A Frontier Orbital Approach. Journal of Physical Chemistry C, 2021, 125, 3827-3844.	3.1	18

Τακάςτι Τογάο

#	Article	IF	CITATIONS
37	Single-Atom High-Valent Fe(IV) for Promoted Photocatalytic Nitrogen Hydrogenation on Porous TiO <sub>2</sub> -SiO <sub>2</sub> . ACS Catalysis, 2021, 11, 4362-4371.	11.2	70
38	Catalytic Methylation of <i>m</i> -Xylene, Toluene, and Benzene Using CO <sub>2</sub> and H <sub>2</sub> over TiO <sub>2</sub> -Supported Re and Zeolite Catalysts: Machine-Learning-Assisted Catalyst Optimization. ACS Catalysis, 2021, 11, 5829-5838.	11.2	25
39	In Situ/Operando IR and Theoretical Studies on the Mechanism of NH <sub>3</sub> –SCR of NO/NO <sub>2</sub> over H–CHA Zeolites. Journal of Physical Chemistry C, 2021, 125, 13889-13899.	3.1	23
40	Analysis of Updated Literature Data up to 2019 on the Oxidative Coupling of Methane Using an Extrapolative Machine‣earning Method to Identify Novel Catalysts. ChemCatChem, 2021, 13, 3636-3655.	3.7	33
41	Roles of the basic metals La, Ba, and Sr as additives in Al2O3-supported Pd-based three-way catalysts. Journal of Catalysis, 2021, 400, 387-396.	6.2	25
42	Analogous Mechanistic Features of NH <sub>3</sub> -SCR over Vanadium Oxide and Copper Zeolite Catalysts. ACS Catalysis, 2021, 11, 11180-11192.	11.2	33
43	Mechanism of NH <sub>3</sub> –Selective Catalytic Reduction (SCR) of NO/NO <sub>2</sub> (Fast SCR) over Cu-CHA Zeolites Studied by <i>In Situ/Operando</i> Infrared Spectroscopy and Density Functional Theory. Journal of Physical Chemistry C, 2021, 125, 21975-21987.	3.1	21
44	Lean NO <i>x</i> Reduction by In-Situ-Formed NH <sub>3</sub> under Periodic Lean/Rich Conditions over Rhodium-Loaded Al-Rich Beta Zeolites. ACS Catalysis, 2021, 11, 12293-12300.	11.2	8
45	Lean NO <sub><i>x</i></sub> Capture and Reduction by NH <sub>3</sub> <i>via</i> NO <sup>+</sup> Intermediates over H-CHA at Room Temperature. Journal of Physical Chemistry C, 2021, 125, 1913-1922.	3.1	15
46	Selective catalytic reduction of NO over Cu-AFX zeolites: mechanistic insights from <i>in situ</i> / <i>operando</i> spectroscopic and DFT studies. Catalysis Science and Technology, 2021, 11, 4459-4470.	4.1	6
47	Synthesis of Zeolitic Ti, Zr-Substituted Vanadotungstates and Investigation of Their Catalytic Activities for Low Temperature NH <sub>3</sub> -SCR. ACS Catalysis, 2021, 11, 14016-14025.	11.2	7
48	High-silica Hβ zeolite catalyzed methanolysis of triglycerides to form fatty acid methyl esters (FAMEs). Fuel Processing Technology, 2020, 197, 106204.	7.2	17
49	Formation and Reactions of NH <sub>4</sub> NO <sub>3</sub> during Transient and Steady-State NH <sub>3</sub> -SCR of NO <sub><i>x</i></sub> over H-AFX Zeolites: Spectroscopic and Theoretical Studies. ACS Catalysis, 2020, 10, 2334-2344.	11.2	67
50	Design of Fe-MOF-bpdc deposited with cobalt oxide (CoOx) nanoparticles for enhanced visible-light-promoted water oxidation reaction. Research on Chemical Intermediates, 2020, 46, 2003-2015.	2.7	4
51	Machine Learning for Catalysis Informatics: Recent Applications and Prospects. ACS Catalysis, 2020, 10, 2260-2297.	11.2	309
52	Promotional Effect of La in the Three-Way Catalysis of La-Loaded Al <sub>2</sub> O <sub>3</sub> -Supported Pd Catalysts (Pd/La/Al <sub>2</sub> O <sub>3</sub> ). ACS Catalysis, 2020, 10, 1010-1023.	11.2	46
53	A CHA zeolite supported Ga-oxo cluster for partial oxidation of CH4 at room temperature. Catalysis Today, 2020, 352, 118-126.	4.4	13
54	Thermally Induced Transformation of Sb-Containing Trigonal Mo <sub>3</sub> VO <sub><i>x</i></sub> to Orthorhombic Mo <sub>3</sub> VO <sub><i>x</i></sub> and Its Effect on the Catalytic Ammoxidation of Propane. Chemistry of Materials, 2020, 32, 1506-1516.	6.7	8

Τακάσηι Τογάο

#	Article	lF	CITATIONS
55	Coordinated Water as New Binding Sites for the Separation of Light Hydrocarbons in Metal–Organic Frameworks with Open Metal Sites. ACS Applied Materials & Interfaces, 2020, 12, 9448-9456.	8.0	11
56	In-Exchanged CHA Zeolites for Selective Dehydrogenation of Ethane: Characterization and Effect of Zeolite Framework Type. Catalysts, 2020, 10, 807.	3.5	14
57	Changes in Surface Oxygen Vacancy Formation Energy at Metal/Oxide Perimeter Sites: A Systematic Study on Metal Nanoparticles Deposited on an In <sub>2</sub> O <sub>3</sub> (111) Support. Journal of Physical Chemistry C, 2020, 124, 27621-27630.	3.1	22
58	The design and development of MOF photocatalysts and their applications for water-splitting reaction. , 2020, , 323-338.		1
59	Frontier Molecular Orbital Based Analysis of Solid–Adsorbate Interactions over Group 13 Metal Oxide Surfaces. Journal of Physical Chemistry C, 2020, 124, 15355-15365.	3.1	22
60	Isolated Indium Hydrides in CHA Zeolites: Speciation and Catalysis for Nonoxidative Dehydrogenation of Ethane. Journal of the American Chemical Society, 2020, 142, 4820-4832.	13.7	86
61	<i>In Situ</i> Spectroscopic Studies on the Redox Cycle of NH <sub>3</sub> â^'SCR over Cuâ^'CHA Zeolites. ChemCatChem, 2020, 12, 3050-3059.	3.7	64
62	Selective C3-alkenylation of oxindole with aldehydes using heterogeneous CeO2 catalyst. Chinese Journal of Catalysis, 2020, 41, 970-976.	14.0	9
63	Mechanistic insights into the oxidation of copper( <scp>i</scp> ) species during NH <sub>3</sub> -SCR over Cu-CHA zeolites: a DFT study. Catalysis Science and Technology, 2020, 10, 3586-3593.	4.1	25
64	Surface Oxygen Vacancy Formation Energy Calculations in 34 Orientations of β-Ga <sub>2</sub> O <sub>3</sub> and θ-Al <sub>2</sub> O <sub>3</sub> . Journal of Physical Chemistry C, 2020, 124, 10509-10522.	3.1	19
65	Catalytic Methylation of Aromatic Hydrocarbons using CO <sub>2</sub> /H <sub>2</sub> over Re/TiO <sub>2</sub> and Hâ€MOR Catalysts. ChemCatChem, 2020, 12, 2215-2220.	3.7	24
66	Machine Learning Predictions of Adsorption Energies of CH4-Related Species. , 2020, , 135-149.		0
67	Esterification of Tertiary Amides by Alcohols Through Câ^N Bond Cleavage over CeO <sub>2</sub> . ChemCatChem, 2019, 11, 449-456.	3.7	21
68	Linear Correlations between Adsorption Energies and HOMO Levels for the Adsorption of Small Molecules on TiO <sub>2</sub> Surfaces. Journal of Physical Chemistry C, 2019, 123, 20988-20997.	3.1	23
69	A Cu–Pd single-atom alloy catalyst for highly efficient NO reduction. Chemical Science, 2019, 10, 8292-8298.	7.4	105
70	Statistical Analysis and Discovery of Heterogeneous Catalysts Based on Machine Learning from Diverse Published Data. ChemCatChem, 2019, 11, 4537-4547.	3.7	54
71	Heterogeneous Pt and MoO <sub><i>x</i></sub> Co-Loaded TiO <sub>2</sub> Catalysts for Low-Temperature CO <sub>2</sub> Hydrogenation To Form CH <sub>3</sub> OH. ACS Catalysis, 2019, 9, 8187-8196.	11.2	66
72	Direct Phenolysis Reactions of Unactivated Amides into Phenolic Esters Promoted by a Heterogeneous CeO 2 Catalyst. Chemistry - A European Journal, 2019, 25, 10515-10515.	3.3	0

Τακάς Ηι Τογάο

#	Article	IF	CITATIONS
73	Formation of Highly Active Superoxide Sites on CuO Nanoclusters Encapsulated in SAPO-34 for Catalytic Selective Ammonia Oxidation. ACS Catalysis, 2019, 9, 10398-10408.	11.2	39
74	Statistical Analysis and Discovery of Heterogeneous Catalysts Based on Machine Learning from Diverse Published Data. ChemCatChem, 2019, 11, 4445-4445.	3.7	6
75	Acetalization of glycerol with ketones and aldehydes catalyzed by high silica Hβ zeolite. Molecular Catalysis, 2019, 479, 110608.	2.0	20
76	Bulk Vanadium Oxide versus Conventional V <sub>2</sub> O <sub>5</sub> /TiO <sub>2</sub> : NH <sub>3</sub> –SCR Catalysts Working at a Low Temperature Below 150 °C. ACS Catalysis, 2019, 9, 9327-9331.	11.2	82
77	Mechanistic study of the selective hydrogenation of carboxylic acid derivatives over supported rhenium catalysts. Catalysis Science and Technology, 2019, 9, 5413-5424.	4.1	25
78	Direct Phenolysis Reactions of Unactivated Amides into Phenolic Esters Promoted by a Heterogeneous CeO <sub>2</sub> Catalyst. Chemistry - A European Journal, 2019, 25, 10594-10605.	3.3	17
79	Experimental and theoretical study of multinuclear indium–oxo clusters in CHA zeolite for CH <sub>4</sub> activation at room temperature. Physical Chemistry Chemical Physics, 2019, 21, 13415-13427.	2.8	18
80	Innentitelbild: MOFâ€onâ€MOF: Oriented Growth of Multiple Layered Thin Films of Metal–Organic Frameworks (Angew. Chem. 21/2019). Angewandte Chemie, 2019, 131, 6856-6856.	2.0	1
81	Design of Pd-based pseudo-binary alloy catalysts for highly active and selective NO reduction. Chemical Science, 2019, 10, 4148-4162.	7.4	41
82	Selective Transformations of Triglycerides into Fatty Amines, Amides, and Nitriles by using Heterogeneous Catalysis. ChemSusChem, 2019, 12, 3115-3125.	6.8	25
83	MOFâ€onâ€MOF: Oriented Growth of Multiple Layered Thin Films of Metal–Organic Frameworks. Angewandte Chemie, 2019, 131, 6960-6964.	2.0	37
84	MOFâ€onâ€MOF: Oriented Growth of Multiple Layered Thin Films of Metal–Organic Frameworks. Angewandte Chemie - International Edition, 2019, 58, 6886-6890.	13.8	145
85	Low-Temperature Hydrogenation of CO <sub>2</sub> to Methanol over Heterogeneous TiO <sub>2</sub> -Supported Re Catalysts. ACS Catalysis, 2019, 9, 3685-3693.	11.2	82
86	N-Methylation of amines and nitroarenes with methanol using heterogeneous platinum catalysts. Journal of Catalysis, 2019, 371, 47-56.	6.2	48
87	Catalytic Activity of Rhodium Phosphide for Selective Hydrodeoxygenation of Phenol. Chemistry Letters, 2019, 48, 471-474.	1.3	6
88	Esterification of Tertiary Amides by Alcohols Through Câ^'N Bond Cleavage over CeO 2. ChemCatChem, 2019, 11, 15-15.	3.7	0
89	Lewis Acid Catalysis of Nb <sub>2</sub> O <sub>5</sub> for Reactions of Carboxylic Acid Derivatives in the Presence of Basic Inhibitors. ChemCatChem, 2019, 11, 383-396.	3.7	53
90	<i>C</i> -Methylation of Alcohols, Ketones, and Indoles with Methanol Using Heterogeneous Platinum Catalysts. ACS Catalysis, 2018, 8, 3091-3103.	11.2	85

Τακάς Ηι Τογάο

#	Article	IF	CITATIONS
91	Water oxidation reaction promoted by MIL-101(Fe) photoanode under visible light irradiation. Research on Chemical Intermediates, 2018, 44, 4755-4764.	2.7	10
92	Toward Effective Utilization of Methane: Machine Learning Prediction of Adsorption Energies on Metal Alloys. Journal of Physical Chemistry C, 2018, 122, 8315-8326.	3.1	140
93	Direct Synthesis of Lactams from Keto Acids, Nitriles, and H <sub>2</sub> by Heterogeneous Pt Catalysts. ChemCatChem, 2018, 10, 789-795.	3.7	28
94	Combined theoretical and experimental study on alcoholysis of amides on CeO2 surface: A catalytic interplay between Lewis acid and base sites. Catalysis Today, 2018, 303, 256-262.	4.4	13
95	Catalytic NO–CO Reactions over La-Al <sub>2</sub> O <sub>3</sub> Supported Pd: Promotion Effect of La. Chemistry Letters, 2018, 47, 1036-1039.	1.3	17
96	The Catalytic Reduction of Carboxylic Acid Derivatives and CO <sub>2</sub> by Metal Nanoparticles on Lewisâ€Acidic Supports. Chemical Record, 2018, 18, 1374-1393.	5.8	18
97	Density Functional Theory Calculations of Oxygen Vacancy Formation and Subsequent Molecular Adsorption on Oxide Surfaces. Journal of Physical Chemistry C, 2018, 122, 29435-29444.	3.1	103
98	Origin of Nb2 O5 Lewis Acid Catalysis for Activation of Carboxylic Acids in the Presence of a Hard Base. ChemPhysChem, 2018, 19, 2809-2809.	2.1	0
99	Acceptorless Dehydrogenative Synthesis of Pyrimidines from Alcohols and Amidines Catalyzed by Supported Platinum Nanoparticles. ACS Catalysis, 2018, 8, 11330-11341.	11.2	58
100	High-silica Hβ zeolites for catalytic hydration of hydrophobic epoxides and alkynes in water. Journal of Catalysis, 2018, 368, 145-154.	6.2	26
101	Acceptorless dehydrogenative coupling reactions with alcohols over heterogeneous catalysts. Green Chemistry, 2018, 20, 2933-2952.	9.0	114
102	Design of Interfacial Sites between Cu and Amorphous ZrO <sub>2</sub> Dedicated to CO <sub>2</sub> -to-Methanol Hydrogenation. ACS Catalysis, 2018, 8, 7809-7819.	11.2	159
103	Origin of Nb <sub>2</sub> O <sub>5</sub> Lewis Acid Catalysis for Activation of Carboxylic Acids in the Presence of a Hard Base. ChemPhysChem, 2018, 19, 2848-2857.	2.1	28
104	Heterogeneous Platinum Catalysts for Direct Synthesis of Trimethylamine by <i>N</i> -Methylation of Ammonia and Its Surrogates with CO <sub>2</sub> /H <sub>2</sub> . Chemistry Letters, 2017, 46, 68-70.	1.3	19
105	Hydrodeoxygenation of Fatty Acids, Triglycerides, and Ketones to Liquid Alkanes by a Pt–MoO <sub><i>x</i></sub> /TiO <sub>2</sub> Catalyst. ChemCatChem, 2017, 9, 2822-2827.	3.7	53
106	Oxidantâ€free Dehydrogenation of Glycerol to Lactic Acid by Heterogeneous Platinum Catalysts. ChemCatChem, 2017, 9, 2816-2821.	3.7	26
107	Fe <sub>3</sub> O <sub>4</sub> @HKUST-1 and Pd/Fe <sub>3</sub> O <sub>4</sub> @HKUST-1 as magnetically recyclable catalysts prepared via conversion from a Cu-based ceramic. CrystEngComm, 2017, 19, 4201-4210.	2.6	28
108	Heterogeneous catalysts for the cyclization of dicarboxylic acids to cyclic anhydrides as monomers for bioplastic production. Green Chemistry, 2017, 19, 3238-3242.	9.0	22

Τακάς Ηι Τογάο

#	Article	IF	CITATIONS
109	TiO2 -Supported Re as a General and Chemoselective Heterogeneous Catalyst for Hydrogenation of Carboxylic Acids to Alcohols. Chemistry - A European Journal, 2017, 23, 980-980.	3.3	3
110	Rhenium‣oaded TiO <sub>2</sub> : A Highly Versatile and Chemoselective Catalyst for the Hydrogenation of Carboxylic Acid Derivatives and the Nâ€Methylation of Amines Using H <sub>2</sub> and CO <sub>2</sub> . Chemistry - A European Journal, 2017, 23, 14848-14859.	3.3	76
111	TiO <sub>2</sub> ‣upported Re as a General and Chemoselective Heterogeneous Catalyst for Hydrogenation of Carboxylic Acids to Alcohols. Chemistry - A European Journal, 2017, 23, 1001-1006.	3.3	45
112	Acceptorless dehydrogenation of N -heterocycles by supported Pt catalysts. Catalysis Today, 2017, 281, 507-511.	4.4	38
113	Supported rhenium nanoparticle catalysts for acceptorless dehydrogenation of alcohols: structure–activity relationship and mechanistic studies. Catalysis Science and Technology, 2016, 6, 5864-5870.	4.1	24
114	Metal–Organic Framework (MOF) and Porous Coordination Polymer (PCP)-Based Photocatalysts. Nanostructure Science and Technology, 2016, , 479-489.	0.1	3
115	Lewis Acid-Promoted Heterogeneous Platinum Catalysts for Hydrogenation of Amides to Amines. ChemistrySelect, 2016, 1, 736-740.	1.5	42
116	Construction of Pt complex within Zr-based MOF and its application for hydrogen production under visible-light irradiation. Research on Chemical Intermediates, 2016, 42, 7679-7688.	2.7	32
117	Catalytic hydrolysis of hydrophobic esters on/in water by high-silica large pore zeolites. Journal of Catalysis, 2016, 344, 741-748.	6.2	18
118	An in situ porous cuprous oxide/nitrogen-rich graphitic carbon nanocomposite derived from a metal–organic framework for visible light driven hydrogen evolution. Journal of Materials Chemistry A, 2016, 4, 18037-18042.	10.3	27
119	NH3-efficient ammoxidation of toluene by hydrothermally synthesized layered tungsten-vanadium complex metal oxides. Journal of Catalysis, 2016, 344, 346-353.	6.2	24
120	Synthesis of 2,5-disubstituted pyrroles via dehydrogenative condensation of secondary alcohols and 1,2-amino alcohols by supported platinum catalysts. Organic Chemistry Frontiers, 2016, 3, 846-851.	4.5	35
121	Visible-light-driven photocatalytic water oxidation catalysed by iron-based metal–organic frameworks. Chemical Communications, 2016, 52, 5190-5193.	4.1	96
122	Design of Zeolitic Imidazolate Framework Derived Nitrogenâ€Doped Nanoporous Carbons Containing Metal Species for Carbon Dioxide Fixation Reactions. ChemSusChem, 2015, 8, 3905-3912.	6.8	53
123	Zeolitic imidazolate frameworks as heterogeneous catalysts for a one-pot P–C bond formation reaction via Knoevenagel condensation and phospha-Michael addition. RSC Advances, 2015, 5, 24687-24690.	3.6	27
124	Positioning of the HKUST-1 metal–organic framework (Cu <sub>3</sub> (BTC) <sub>2</sub> ) through conversion from insoluble Cu-based precursors. Inorganic Chemistry Frontiers, 2015, 2, 434-441.	6.0	54
125	Immobilization of Cu Complex into Zr-Based MOF with Bipyridine Units for Heterogeneous Selective Oxidation. Journal of Physical Chemistry C, 2015, 119, 8131-8137.	3.1	89
126	Visible-light, photoredox catalyzed, oxidative hydroxylation of arylboronic acids using a metal–organic framework containing tetrakis(carboxyphenyl)porphyrin groups. Chemical Communications, 2015, 51, 16103-16106.	4.1	93

Τακάςτι Τογάο

#	Article	IF	CITATIONS
127	Development of a novel one-pot reaction system utilizing a bifunctional Zr-based metal–organic framework. Catalysis Science and Technology, 2014, 4, 625.	4.1	63
128	Development of a Ru complex-incorporated MOF photocatalyst for hydrogen production under visible-light irradiation. Chemical Communications, 2014, 50, 6779.	4.1	145
129	Enhanced photoelectrochemical properties of visible light-responsive TiO2 photoanode for separate-type Pt-free photofuel cells by Rh3+ addition. Research on Chemical Intermediates, 2013, 39, 1603-1611.	2.7	4
130	Efficient hydrogen production and photocatalytic reduction of nitrobenzene over a visible-light-responsive metal–organic framework photocatalyst. Catalysis Science and Technology, 2013, 3, 2092.	4.1	198
131	Application of an amino-functionalised metal–organic framework: an approach to a one-pot acid–base reaction. RSC Advances, 2013, 3, 21582.	3.6	67
132	FT-IR study of the reaction mechanisms for photocatalytic reduction of NO with CO promoted by various single-site photocatalysts. Journal of Catalysis, 2013, 299, 232-239.	6.2	9
133	Development of dye-sensitized solar cells based on visible-light-responsive TiO2 thin films with a unique columnar structure. Research on Chemical Intermediates, 2013, 39, 415-424.	2.7	6
134	Effect of pore sizes on catalytic activities of arenetricarbonyl metal complexes constructed within Zr-based MOFs. Dalton Transactions, 2013, 42, 9444.	3.3	37
135	Recent advances in visible-light-responsive photocatalysts for hydrogen production and solar energy conversion – from semiconducting TiO2 to MOF/PCP photocatalysts. Physical Chemistry Chemical Physics, 2013, 15, 13243.	2.8	139
136	Visible-Light-Promoted Photocatalytic Hydrogen Production by Using an Amino-Functionalized Ti(IV) Metal–Organic Framework. Journal of Physical Chemistry C, 2012, 116, 20848-20853.	3.1	551